Colloids and Surfaces A: Physicochemical and Engineering Aspects 698 (2024) 134528

Contents lists available at ScienceDirect

Colloids and Surfaces A: Physicochemical and Engineering Aspects

journal homepage: www.elsevier.com/locate/colsurfa

# Tailoring the properties of castor oil polyurethanes organogels with green oligoesters

D. Bandelli [a], R. Mastrangelo [a], G. Poggi [b], D. Chelazzi [b,*], P. Baglioni [b]

[a] Department of Chemistry, University of Florence, Via della Lastruccia 3, Sesto Fiorentino, FI 50019, Italy
[b] Department of Chemistry and CSGI, University of Florence, Via della Lastruccia 3, Sesto Fiorentino, FI 50019, Italy

## GRAPHICAL ABSTRACT

**The use of "green" oligoester additives in the design of castor oil-polyurethanes allows control of the gelation process, tuning micro- and nanostructural features, and solvent entrapment. Herein, the new castor oil-oligoester organogels are thoroughly characterized and tested as tools for the cleaning of artifacts and cultural heritage preservation.**

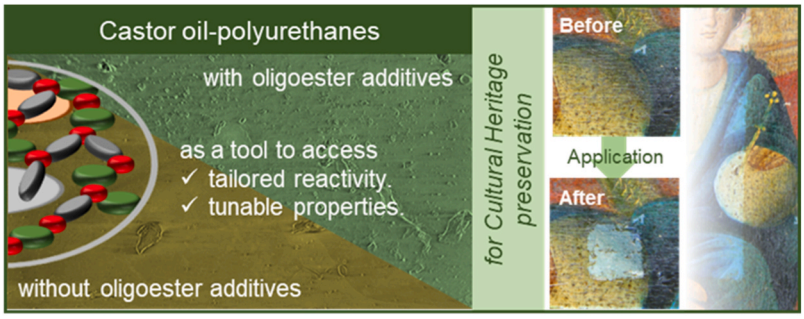


## ARTICLE INFO

*Keywords:*
Castor oil
Polyurethanes
Polyesters
Microstructure
Nanostructure
Solvent entrapment

## ABSTRACT

Castor oil (CO) can react with isocyanate to form polyurethane organogels, whose hydrophobicity can be regulated by functionalization with "green" oligoesters of bio-dicarboxylic acids. Here, we elucidated the gelation mechanism induced by the oligoesters to gain control of the gels' mechanical properties and solvent confinement capacity. This can be useful in cleaning Cultural Heritage items, a socioeconomically important application, and other scientific/technological sectors. During gelation, the oligoesters react with isocyanate to form aggregates whose compatibility with CO is regulated by the oligoesters' hydrophobicity. This allows fine control of gelation time and of the gels' micro- and nanostructure structure, where the presence of oligoesters in solid-like regions regulates rheological behaviour and mechanical resistance. The gels' solvent upload capacity also depends on the oligoesters' hydrophobicity, which can favour chain relaxation over Fickian diffusion during

*Abbreviations:* CO, castor oil; DOSY, diffusion ordered spectroscopy; NMR, nuclear magnetic resonance; CH, Cultural Heritage; VOCs, volatile organic compounds; $M_n$, number-average molar masses; Đ, dispersity index; SEC-MALS, size exclusion chromatography-multi angle light scattering; ClogP, calculated octanol/water partition coefficient; *Xc*, melting temperature; $T_m$, degree of crystallinity; DSC, differential scanning calorimetry; WAXS, wide-angle X-ray scattering; SAXS, small-angle X-ray scattering; CO-PUs, castor oil polyurethanes; PHDI, polyhexamethylene diisocyanate; $T_{gel}$, gelation time; $R_h$, hydrodynamic radius; SEM, scanning electron microscopy; CLSM, confocal light scanning microscopy; RBITC, rhodamine B isothiocyanate; FITC, fluorescein isothiocyanate; G', storage modulus; G'', loss modulus; THF, tetrahydrofuran; MEK, methyl ethyl ketone, DEC, diethyl carbonate; R/F, relaxation/fickian ratio.

* Corresponding author.
*E-mail address:* david.chelazzi@unifi.it (D. Chelazzi).

https://doi.org/10.1016/j.colsurfa.2024.134528
Received 8 May 2024; Received in revised form 7 June 2024; Accepted 11 June 2024
Available online 12 June 2024

swelling. Finally, the swollen organogels were used to remove organic varnishes/coatings from painted wood and glass, demonstrating potential as sustainable cleaning tools for works of art.

## 1. Introduction

Smart advanced materials represent one of the most intriguing topics in material science, as they enable solving complex functions, with higher time-effectiveness and improved sustainability than traditional benchmarks [1–5]. In particular, versatile materials with potential application in multiple scientific and technological sectors are advantageous, and key desirable characteristics comprise the ability to respond in controlled ways to external stimuli such as temperature or the presence of chemicals, self-healing materials, etc. [6–14]. Examples of fields where such responsive materials are continuously researched and developed include food industry [15], cosmetics [16], biomedicine [17], agriculture [18], tissue engineering [19], and even the preservation of Cultural Heritage (CH) [20–22], where smart materials allow the durable restoration of works of art, buildings and collections, boosting their socioeconomic value [23–26]. Indeed, while the traditional practice in CH preservation has borrowed materials and concepts from industrial applications, in the last decades research in art conservation science has produced solutions with potential impact in several fields. In this sense, colloids and soft matter have proven to be an ideal framework to devise advanced materials with enhanced properties, such as physical and chemical gels [27–31].

Namely, gels are optimal tools to address the preservation of canvas paintings, iconic artifacts that hold fundamental historical, artistic, and economic value. One of the most recurring tasks is the removal of soil, aged coatings, adhesives and varnishes, or vandalism, from the paintings surface. Owing to the presence of water- and solvent-sensitive pigments, dyes, binders and additives, both classic and modern/contemporary paintings can be highly challenging and risky to clean with conventional solvent blends and aqueous solutions [32–34]. The confinement of cleaning fluids in retentive matrices, then, can allow safe cleaning interventions, provided that these matrices are retentive and exhibit good mechanical properties.

Both hydro- and organogels have been formulated over the decades to confine, respectively, aqueous fluids [35] or organic solvents, with improved control and performances over traditional polymeric thickeners. Moreover, the gels' apparent tortuosity has been successfully linked to the systems' cleaning performance [36,37].

However, while hydrogels have been demonstrated for the cleaning of paintings such as works of Pablo Picasso [38], Jackson Pollock [39], and others [40,41], organogels are still in their infancy, and only limited materials and synthetic approaches have been explored [42–45]. Because modern/contemporary paintings are often highly water-sensitive [32–34], the development of valid organogels remains an open issue in CH conservation. In addition to effectiveness, a fundamental requirement is that newly developed materials must be sustainable and exhibit a high green chemistry profile with reduced toxicity and ecological impact [36,37,46,47,48], coping with international policies such as the European Green Deal [49,50]. For instance, chemical organogels based on polymethacrylates have been previously demonstrated [51–53], but they are often restricted to solvents with average polarity, and are derived from petrochemical resources.

In this regard, castor oil (CO) represents a strategic building block for material preparation due to its renewability and biodegradation [54,55]. In addition, CO does not impact on the food chain, and can be grown in marginal lands [56–59]. Taking advantage on the reactivity of ricinolein, the major CO component, polyurethanes can be feasibly obtained to build organogel networks [60–62]. One of the key features of this approach is that CO-gels can be obtained directly as dry systems that can be easily stored, and then loaded with solvents before application [63]. Alternatively, these CO-based polyurethane networks can also be uploaded with particles to capture and neutralize volatile organic compounds (VOCs) in the preventive conservation of museum enclosures [64]. In addition, the polyurethane network can be built by reacting CO with a bio-derived isocyanate, whose improved hydrophilicity provides the gel with good biodegradability in soil and compost [65].

However, despite these promising characteristics, several physicochemical aspects of this CO organogel class are still poorly explored. Careful evaluation and control of the CO-gel synthetic pathways is required to tune solvent entrapment, a major feature in several applications. In principle, the use of additives can control structural features of the polyurethane network at the micro and nanoscale, tailoring its macroscopic features in addition to solvent confinement and release. Recently, we have reported on the preparation of a library of oligoesters, derived from bio-dicarboxylic acids, as probes for a new protocol to evaluate polymers/oligomers hydrophobicity estimation, and the application of the protocol to predict solvents compatibility in gelled polymer systems [66]. While these "green" oligoesters can be used to enrich CO gels, the gelation mechanisms induced by the esters was not yet understood, and their specific effect on the gels' structure and uploaded solvent dynamics was not studied. These are crucial aspects to control the gels' properties and boost their versatility and applicative potential.

Herein we study the correlation among the oligoesters hydrophobicity, the formation of a polyurethane CO-isocyanate-oligoester three-dimensional network, and the final properties of these new CO organogels. Aiming to obtain the polyurethanes without the addition of solvents, a synthetic protocol in melt was established. The study of the gelation process through rheology and nuclear magnetic resonance shed light on the central role of the oligoesters hydrophobicity during gel formation. Extensive characterization was carried out on the final gel materials, through scanning electron and confocal microscopy, small-angle X-Ray scattering, and rheology, to link the gelation mechanism with the structural features of the gels. Then, aiming to test the gels in art cleaning applications, solvent upload was studied with a series of solvents with varied hydrophilic/hydrophobic balance, analyzing different swelling behaviors. Finally, application of the CO gels on model surfaces was performed to remove coatings and varnishes found in the restoration practice.

## 2. Results and discussion

### 2.1. Oligoester synthesis and properties

The synthesis of oligoesters employed as additives for the preparation of castor oil-polyurethane systems was accomplished according to a previously reported procedure [66]. Briefly, a two-step polycondensation reaction of selected dicarboxylic acids (sebacic acid, adipic acid or succinic acid) and diols (hexanediol or butanediol) was performed at 180 °C. As a result, the library of oligoesters **O1** to **O5** featured similar number-average molar masses ($M_n$) and moderate dispersity index (Đ) according to size exclusion chromatography-multi angle light scattering (SEC-MALS) analysis (Table 1).

Before employing the oligoester library as additives in castor oil-polyurethanes networks, bulk properties such as melting temperatures ($T_m$) and degree of crystallinity (*Xc*) were investigated by means of differential scanning calorimetry (DSC) and wide-angle X-ray scattering (WAXS). DSC analyses were performed in a temperature range between – 80 and 150 °C using two consecutive heating/cooling runs. During the first heating run, the oligoester with the highest repetition unit clogP, *i.e.* the calculated water/octanol partition coefficient, (**O1**, 4.57) featured a

**Table 1**
Selected structural characterization data of the synthesized oligoesters [66].

| Code | Repetition unit | clogP[a] | $M_n$ [kg mol$^{-1}$][b] | Đ[b] | $T_m$ [°C] | $X_c$ [%] |
|---|---|---|---|---|---|---|
| **O1** | hexylene sebaceate | 4.57 | 3.0 | 1.36 | 67.9 | 67.5 |
| **O2** | butylene sebaceate | 3.66 | 3.0 | 1.37 | 63.6 | 62.8 |
| **O3** | hexylene adipate | 2.75 | 2.8 | 1.48 | 58.2 | 56.6 |
| **O4** | hexylene succinate | 1.84 | 3.0 | 1.42 | 53.4 | 49.5 |

[a] Octanol/water partition coefficient calculated from the meric structure with OSIRIS DataWarrior (v. 5.5.0) [67].
[b] Number-average molar mass ($M_n$) and dispersity index (Đ) obtained with absolute calibration (Viscometer-RI detection) by SEC-MALS analysis, THF, 40 °C, 1 mL min$^{-1}$. The melting temperatures ($T_m$) and degree of crystallinity (*Xc*) were obtained here by DSC and WAXS measurements.

melting point at 67.9 °C (Fig. 1). When clogP decreases passing from **O1** to **O4**, $T_m$ decreased linearly, suggesting that the different chemical structure of the repetition units (meric) could impair the formation of crystalline domains in the pure oligoester samples in line with literature data on similar systems [68–71]. The second heating run confirmed that the same trend of $T_m$ *vs.* clogP occurs also when the thermal history is removed. Exothermic crystallization events, occurring during the first cooling run, follow the same trend as for $T_m$ (see Fig. 1).

Interestingly, similar WAXS patterns were collected on all the oligoesters, showing two main peaks at 21.8 and 24.8 2θ, *i.e.* the different meric structure in **O1**-**O4** did not produce a variation in the structure of crystallites. However, the degree of crystallinity showed the same trend than $T_m$, with the highest (67.5 %) for **O1** and the lowest (49.5 %) for **O4**.

Thus, the **O1** to **O4** series constitutes a compact library of oligoesters with similar molar mass but tuned thermal/structural properties (further investigated in the following sections), which was employed as additive for the preparation of the castor oil-oligoester polyurethanes.

### 2.2. The gelation of oligoesters-enriched CO polyurethanes

The oligoesters **Ox** were used in the formulation of castor oil polyurethanes (CO-PUs) employing poly(hexamethylene diisocyanate) (pHDI) as crosslinking agent (CO:**Ox**:pHDI mass feed ratio of 72:10:18) at 80 °C, above the melting temperature of the oligoesters. In addition, CO was also simply reacted with pHDI (CO:pHDI 82:18) as a blank reference gel formulation. Already during the first polymerization tests, the addition of the oligoesters resulted in faster gelation as compared with the blank. Insights on the reaction process were obtained with rheological measurements in viscosity and oscillatory time sweep modes at 80 °C. Briefly, all the samples analysed at this stage were prepared as follows: CO and the selected **Ox** were transferred on a round bottom flask and heated at 80 °C until complete homogenization. Subsequently, pHDI was added to the CO-Ox mixture and the reaction was mixed with a stirring rod for 5 minutes at 80 °C. Afterwards, c.a. 2 mL of the reaction mixture was transferred on the pre-heated plate of the rheometer. Viscosity, measured after 10 and 20 minutes from the reaction onset, is lowest for the blank, while the addition of oligoesters produced a viscosity increase (Figure S2). Interestingly, oscillatory time sweeps showed a trend in gelation time ($t_{gel}$), indicated by the crossover of the system's elastic and viscous moduli, with the fastest formulation

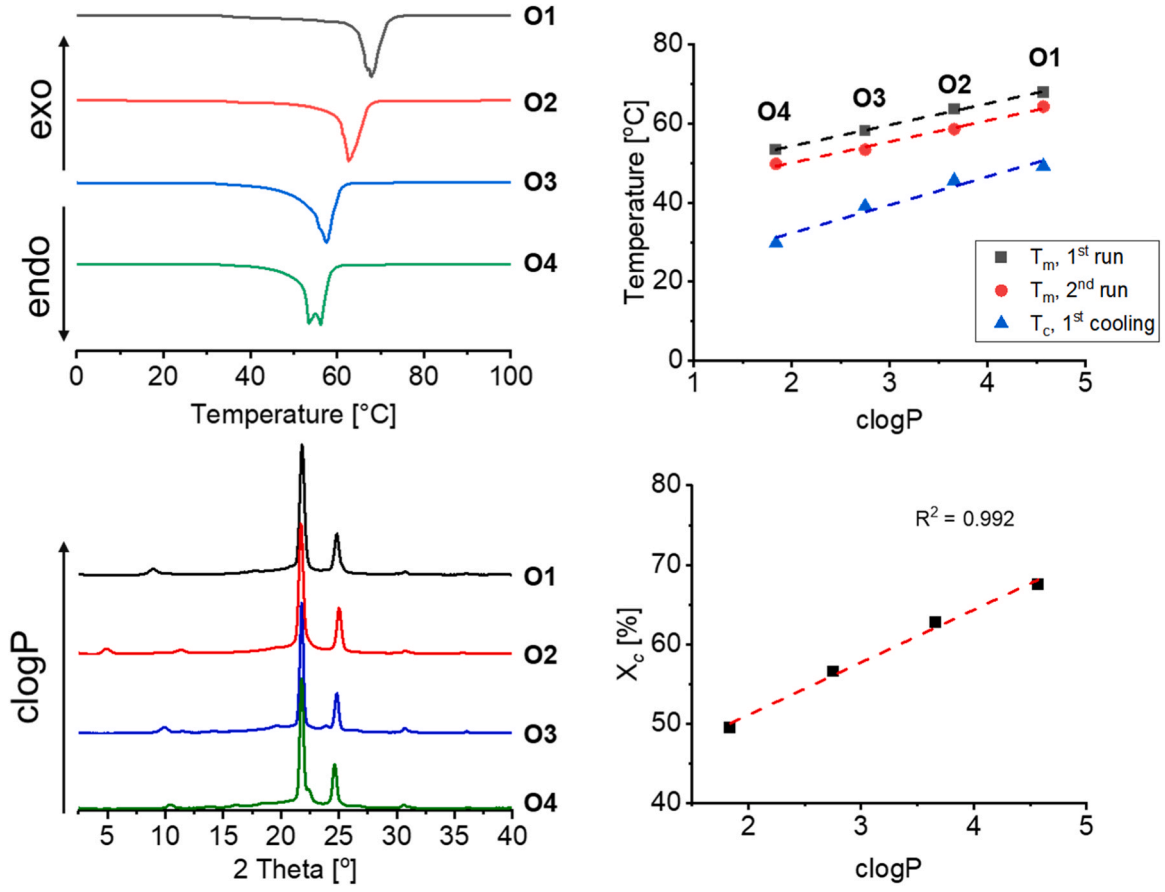


**Fig. 1.** Bulk analysis of the samples **O1** to **O4**. Top Left: First heating run of DSC between 0 and 100°C. Top Right: Plot of melting points ($T_m$) and crystallization temperatures ($T_c$) *vs.* oligoester clogP, obtained respectively during the first and the second heating run, and the first cooling run (cooling runs are depicted in Fig. S1). The dashed lines are guidelines. Bottom Left: WAXS curves of oligoesters **O1** to **O4** at room temperature. Bottom Right: Plot and linear fitting of the degree of crystallinity ($X_c$) *vs.* oligoesters clogP. Errors are included in the markers.

(containing **O2**) reaching $t_{gel}$ in ~45 minutes, and the blank in ~230 minutes (Fig. 2). Overall, the trend in gelation time is **O2** < **O3** ≈ **O1** < **O4**.

Since the oligoesters have similar molar masses but different meric structure, we hypothesized that hydrophobic interactions among the pre-gel components played a major role during gelation. The calculated logP of the oligoester's repetition unit (clogP, see Table 1) was thus chosen as a parameter of each component's hydrophobicity. Notably, there is a large clogP gap between pHDI (3.61) and ricinolein (17.99), the reacting component of castor oil. Instead **O2**, the oligoester that mostly accelerates gelation, has the closest clogP to pHDI. Overall, the evolution of $t_{gel}$ with the clogP deviation from pHDI ($|clogP_{pHDI} - clogP_{Ox}|$) is a non-linear increase with the trend **O2** < **O3** ≈ **O1** < **O4**.

As an additional tool to study the reaction between castor oil, pHDI and **Ox**, DOSY NMR analysis were performed on the separate components and on pre-gel mixtures over 15 minutes since the reaction onset. In all the samples containing the oligoesters, the diffusion plot showed three main diffusion coefficients, related to the signals of species containing mostly either castor oil, pHDI or oligoesters (Fig. 2, Figure S3).

In agreement with the rheological analysis, the addition of oligoesters resulted in faster growth of aggregates in the reacting pre-gel mixtures than in the blank pre-gel (Fig. 2). In detail, the signals of oligoesters-containing aggregates followed the same **O2** > **O3** ≈ **O1** > **O4** trend (Fig. 2), which also follows the match of the oligoesters' clogP with pHDI's. The evolution of the signals related to pHDI- and CO-containing species followed similar trends (Figure S3).

Overall, the combined rheological and NMR analyses suggest that the oligoesters act as compatibilizers for the reaction of CO with pHDI during gelation, and their capability to do so is regulated by their hydrophobicity.

In principle, the reaction between pHDI and **Ox** results in the formation of larger aggregates with increased hydrophobicity, which in turn have higher tendency to incorporate castor oil, the most hydrophobic component of the mixture, in the three-dimensional structure of the forming polyurethane. In fact, clogP calculations of pHDI-Ox aggregates indicated that clogP can be increased up to closely match the logP of ricinolein. Accordingly, and based on our experimental data, the gelation mechanism could be summarized in the following steps (Fig. 3): (i) initial formation of pHDI-**Ox** aggregates; (ii) the aggregates have increased compatibility with CO and thus start to include it in larger structures; (iii) the final network forms, composed of dense regions of CO and **Ox**.

### 2.2.1. *Properties of the oligoesters-enriched CO polyurethanes*

The oligoesters-enriched castor oil polyurethanes were prepared in ~0.2 cm thick sheets, employing a CO:**Ox**:pHDI mass% ratio of 72:10:18. The new gels were labelled **G0** (blank without oligoester), and **G1** to **G4** according to the oligoester employed during the synthesis, *e.g.* **G1** contains 10 m% of **O1**.

While the blank gel **G0** is transparent, the remaining **Gx** are opalescent (see Fig. 4), suggesting the presence of micro-, and possibly, nanodomains likely produced by the phase separation of aggregates during the reaction. All samples have micro-clots >15 $\mu$m distributed across the gels' matrix (Fig. 4) as visualized by scanning electron microscopy (SEM) analysis. Moreover, looking at the gels' vertical section showed that the addition of **Ox** produced a vast number of micro domains of 1–5 $\mu$m. Confocal light scanning microscopy (CLSM) revealed that the large microdomains observed with SEM are oligoester domains (marked in green), that are recurring in the sample, surrounded by a dense region of CO (marked in red), see Fig. 4.

Insights on the polyurethane nanostructure were then obtained by SWAXS (Fig. 5).

In addition to broad peaks related to the gels' characteristic mesh-sizes or interatomic distances, systems **G1** to **G4** showed two main peaks likely due to oligoesters crystallites at 2 theta values close to 22° and 25° (Fig. 5). Interestingly, the degree of crystallinity obtained from the WAXS curves, follows the same trend as gelation speed (**G2** > **G1** ≈ **G3** > **G4**, see Figure S4). This indicates that, in addition to driving the gelation process, the oligoester hydrophobicity also affects the final structure of the gel network.

Characteristic dimensions of the networks at the nanoscale were then obtained through analysis of the SAXS curves. A customized fitting model, which we previously adopted for CO organogels,[63] was adapted to describe the new CO-oligoesters' profiles:

$$I(Q) = I_{Porod}(Q) + I_{Inhomogeneities}(Q) + I_{Gaussian,1}(Q) + I_{Gaussian,2}(Q) + I_{Gaussian,3}(Q) + Bkg \quad (1)$$

The first term in Eq. 1 features a Porod slope at low Q, accounting for the scattering from large clusters of different density:

$$I_{Porod}(Q) = \frac{I_P(0)}{Q^n} \quad (2)$$

where $I_P(0)$ is a constant and n the Porod exponent.

The second term in Eq. 1 is the Guinier function, accounting for the presence of solid-like inhomogeneities in the networks [72]:

$$I_{Inhomogeneities}(Q) = I_G(0) \bullet \exp\left[-\frac{Q^2 \bullet R_g^2}{3}\right] \quad (3)$$

where $I_G(0)$ is the Guinier excess intensity at Q = 0, and $R_G$ the gyration radius of the clusters.

The last terms preceding the background (Bkg) in Eq.1 are gaussian functions, used to model the broad peaks found at high Q in all the gels' curves:

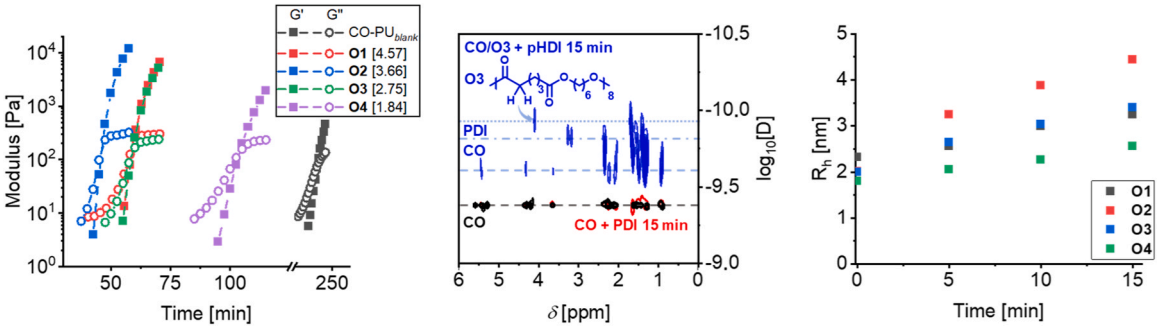


**Fig. 2.** (Left) Oscillatory time sweep experiments to determine gelation time ($t_{gel}$) of the castor oil gels. The coloured dashed lines are guidelines. Errors are included in the markers. (Centre, left) Diffusion of CO (black) and its mixtures with pHDI (red), or with pHDI and **Ox** (blue), obtained via DOSY NMR in deuterated chloroform at 25 °C. Left**:** DOSY NMR plots of CO (black), CO and pHDI (red) and CO, **O3** and pHDI mixtures (blue). The mixtures were quenched after 15 minutes of stirring at 80 °C. Right**:** Plots of the hydrodynamic radii ($R_h$), obtained from the signals related to the **Ox**-containing species, *vs.* reaction time. Errors are included in the markers.

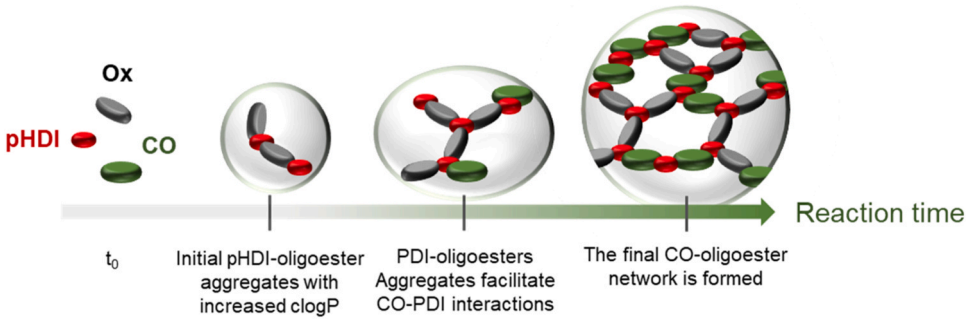


**Fig. 3.** Schematic representation, based on the rheological and NMR data, of the reaction between castor oil, **Ox** and pHDI, to yield CO-oligoester polyurethane gel networks.

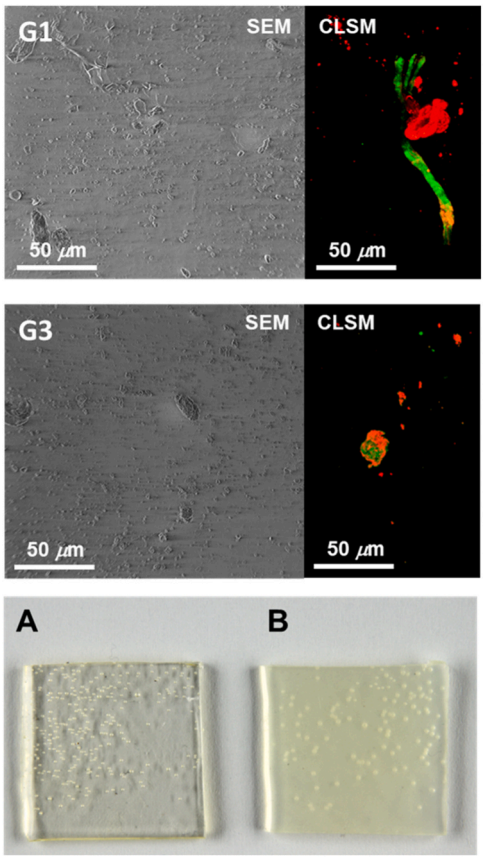


**Fig. 4.** Top. SEM and CLSM images of CO gels **G1** and **G3**. From left to right, SEM analysis of the polyurethane surfaces and CLSM of vertical sections. In CLSM images the RBITC-labelled castor oil is marked in red, while the FITC-labelled **Ox** in green. The CLSM images here reported were corrected to visualize the gel's background as black. For additional SEM analysis see the Supporting Information file. Bottom.(A) A **G0** CO gel (blank without oligoester additive) and (B) a **Gx** CO gel.

$$I_{Gaussian}(Q) = I_{Ga} \bullet \exp\left[-\frac{0.5 \bullet (Q-Q)^2}{\sigma^2}\right] \quad (4)$$

Porod's and Guinier's terms fitting parameters are listed in Table 2.

Inhomogeneity at the nanoscale was not observed from the SAXS curves of **G0**, which is characterized only by a −4 Porod slope that indicates a smooth surface.

In the **Gx** series the radius of gyration, $R_G$, is likely related to solid-like domains composed of polymer aggregates [20,39], in our case oligoesters. While $R_G$ does not vary significantly among **G1**, **G2** and **G3**, its value is substantially smaller in **G4**, which also showed the lowest lower degree of crystallinity in the series. **G4** has also the lowest scale parameter $I_G$, *i.e.* it has fewer solid-like regions. At lower Q, the Porod exponent n describes the presence of large mass fractals, denser in **G2 – G4** than in **G1**.

Peaks in the high-Q range are similar in all gels, characterized by lengths of 27, 12 and 4 Å, respectively (see Q values in Table S1). Such characteristic dimensions are likely related to interatomic distances or characteristic mesh-sizes generated after crosslinking, and not to specific oligoesters (no differences among **G0** and **G1 – G4**).

Overall, from microscopy and X-ray scattering data we concluded that the oligoesters confined in the polyurethane matrix can rearrange during the gel formation process, generating solid-like fractions at the micro- and nanoscale, and the **Ox** hydrophobicity regulates the dimensions of solid-like regions and crystallites in the gels with similar trends as in the gelation speed.

The structural characterization was complemented by the study of the mechanical properties of the CO gels, through frequency sweep experiments (Fig. 6).

Independently of the **Ox** additive used, the storage and loss moduli (G' and G'') are higher in **Gx** than **G0**. In agreement with SWAXS data, G', which describes the gels' solid-like behaviour, followed the trend **G2** ≈ **G1** > **G3** > **G4**, *i.e.* the higher the number and size of solid-like regions, the higher G'. Moreover, G'' shows a similar trend.

Heating up to 80℃ resulted in a decrease of G' for all the samples, ascribed to the melting of the solid-like oligoesters aggregates. The decrease is highest in **G2** (ΔG' ~50 kPa), the sample with the highest crystallinity and solid-like areas, and lowest in **G4** (~6 kPa), which has the lowest crystallinity. Indeed, **G2** shows the highest modulus up to 50°C, and the lowest at 80°C, following the melting of the oligoester domains. The variation of the storage modulus (G') during heating across the **G1**-**G4** series seems to be related to the melting of oligoester chains capable of forming aggregates physically linked and crosslinked to the gel network. Thus, we hypothesized that the oligoester additives can be present either as entangled branched units or involved in the gel's chemical crosslink network (Fig. 6), and the entangled units are capable of crystallizing similarly to the unbound oligoesters. This hypothesis was also suggested by the increase of tan($\delta$) (the G"/ G'ratio) for **G1**-**G4** series passing from 25 to 80°C, *i.e.* physically linked/crosslinked oligoester domains could melt inside gel regions confined by chemical crosslinks. Indeed, it is known in the literature that oligoester units involved in physically linked/crosslinked entanglements affect the rheological behavior of the rubbery network [73–76].

The gels' compatibility with a range of solvents with varied hydrophilic/lipophilic balance (ethanol, acetone, MEK, DEC and *p*-xylene) was then linked to the networks' hydrophobicity *via* swelling experiments. In principle, the solvent uptake capability can give information on the diffusion/swelling mechanism in the three-dimensional structure of rubbers and gels, and on the gels' structure [77–79]. Swelling of **G0** in ethanol (which has logP −0.24) resulted in a plateau in the solvent

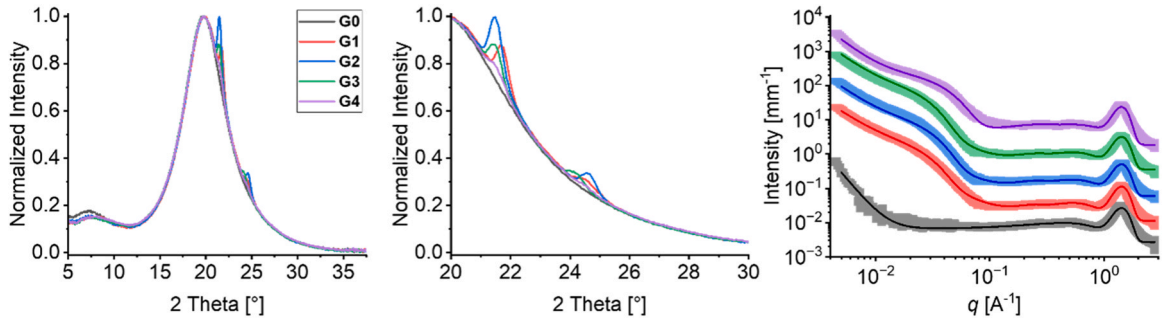


**Fig. 5.** SWAXS profiles of the **G0-4** CO organogels. Left/Centre**.** WAXS profiles and detail of the 20–30° region. Right**.** SAXS curves (dots) and fitting (lines) according to Eqs. 1–4.

**Table 2**
Overview of the Porod's and Guinier's SAXS fitting parameters of gels **G0** – **G4**, obtained from Eq. 1.

| Code | IP [10–6] | n | $I_G$ | $R_G$ [Å] | Bkg |
|---|---|---|---|---|---|
| **G0** | 0.00018 ± 0.00005 | 4.0 ± 0.1 | - | - | 0.003 ± 0.001 |
| **G1** | 20.2 ± 0.1 | 2.39 ± 0.1 | 0.74 | 69 ± 5 | 0.003 ± 0.001 |
| **G2** | 9.30 ± 0.05 | 2.68 ± 0.1 | 1.48 | 72 ± 5 | 0.003 ± 0.001 |
| **G3** | 8.03 ± 0.05 | 2.67 ± 0.1 | 1.10 | 67 ± 5 | 0.003 ± 0.001 |
| **G4** | 2.50 ± 0.05 | 2.60 ± 0.1 | 0.25 | 40 ± 5 | 0.003 ± 0.001 |

uptake ($\Delta m/m_0$) at ≈ 0.7 after 5 h. Lower values (0.5–0.6) were obtained for the **Ox**-containing gels. Increasing the solvent hydrophobicity up to MEK (logP 0.37) gave higher $\Delta m/m_0$, with maximum values between 1.8 and 2.2. However, more hydrophobic solvents reduced the maximum uptake, *i.e.* the overall swelling capability of the **Gx** samples was maximized for solvents with average hydrophobicity. Overall, we expected that different structural features in the **Ox** additives could affect solvent confinement in the corresponding gels. To support this hypothesis, the swelling curves were fitted to the Peppas-Salhin equation, evaluating diffusive and relaxation phenomena in solvent uptake by the polymer network [80–82]:

$$\frac{m}{m}_{t,\infty} = k_F t^m + k_R t^{2m} \quad (5)$$

where $m_t$ is the mass of the solvent uploaded in the gel at time t, $m_\infty$ is the solvent upload at equilibrium (which was reached in variable times from ca. 180–600 minutes), $k_F$ and $k_R$ are the kinetic constants of, respectively, diffusive and relaxation process, and m is the purely Fickian diffusion exponent. According to the model, m decreases from 0.500 to 0.425 as the thickness of the absorber increases upon swelling in the solvent.

The fitting was performed for datapoints with $m_t/m_\infty$ below 0.7 as required from the model. i.e. for the kinetic process before reaching the equilibrium (Fig. 7) [80,83,84].

The obtained values of m depend strongly on the **Ox** employed in the gels' synthesis, and on the solvent choice (Table S2**,** Fig. 7**,** Figure S5).

The fitting results are reported in Table S2. Changing the oligoester additive's clogP in the **Gx** series for different solvents allowed pronounced swelling (up to m = 0.425). An indication of the balance between chain relaxation and pure diffusive phenomena during solvent uptake in the gels, is represented by the Relaxation/Fickian ratio ("R/F"), expressed by [80]:

$$\frac{R}{F} = \frac{k_R}{k_F} t^m \quad (6)$$

that uses the fitting parameters obtained from Eq. 5.

A plot of R/F at 180 minutes *vs.* the clogP of the oligoester additive's **Ox** in the gels, is given in Fig. 7. The results showed that for DEC (logP 1.21) and less hydrophobic solvents, higher R/F values were obtained for **G4**, while **G1** featured the highest R/F value when *p*-xylene (logP 3.15) was uploaded. Therefore, the gels' affinity (relaxation over diffusion) to a range of organic solvents can be tuned by changing the oligoester additive in the CO polyurethane matrix. Overall, we observed that the CO-oligoester gels were able to upload the solvents up to more than 200 % of their initial weight, depending on the mutual additive-solvent chemical affinity. This versatility in solvent uptake could represent an improved practical advantage when the swollen organogels are used to remove varnishes and coatings from works of art.

The capability of the systems **G1** and **G4**, swollen in solvents, to remove typical coatings/varnishes found in art restoration, was then checked. Fig. 8 shows the results of the gels application to a painted wood panel, and to glass. Previous characterization carried out on this wood panel had shown that it has a top layer of a polyhydroxy acid–based varnish (e.g., shellac) [85]. This class of resins is found in varnishes applied onto artifacts [86–88]. The varnish was likely applied to the panel by the artist, or in some past restoration intervention, and has naturally aged over time into a brownish layer that strongly jeopardize the appearance of the artifact. The **G4** organogel was swollen in MEK for 35 minutes, and then shortly applied to the varnished surface, leading to the removal of the varnish and the recovery of the painted layer. Glass was instead chosen as a model surface and coated with beeswax, another coating found on works of art [89–91]. The **G1** organogel was swollen in *p*-xylene for 35 minutes, and then applied onto the coated surface, leading to the removal of wax. The chemical action of the organogel was coupled with gentle mechanical action with a swab to remove the swollen/softened coating. These preliminary tests showed that the new CO-oligoester gels have versatility and potential as tools for further evaluation in cleaning interventions on works of art.

## 3. Conclusion

We elucidated for the first time the gelation mechanism in castor oil (CO) polyurethane networks enriched with a library of "green" oligoesters, obtained from biomolecules (dicarboxylic acids) and diols. In addition, the effect of the esters on the gels' structure, mechanical properties, and solvent upload dynamics, were detailed.

The key-result is that the oligoesters' hydrophobicity, expressed by their clogP parameter (calculated water/1-octanol partition coefficient), regulates the gelation process, allowing fine control of the structure of the obtained networks, and of the gels' capacity to upload solvents of different polarity. In particular, as indicated by rheology and DOSY NMR analysis, the driving force in the CO polyurethane formation is likely the compatibilization of pHDI with castor oil through the formation of hydrophobic oligoester-pHDI units able to incorporate CO as the network builds. In addition, the oligoesters can also rearrange during gelation to generate physically linked solid-like fractions and crystallites, whose dimension increases with the oligoesters' clogP, which increase the elastic modulus of the gels. The oligoesters' clogP can be

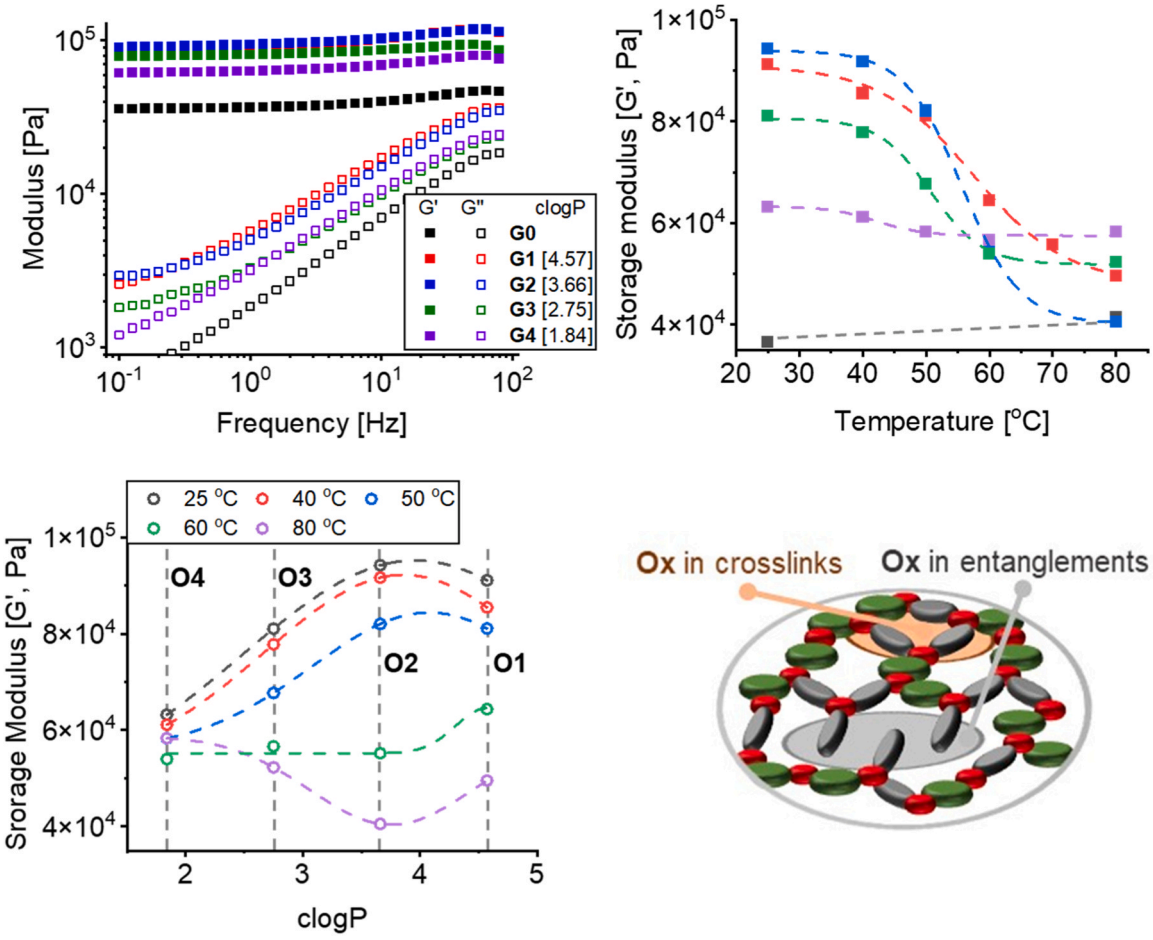


**Fig. 6.** Frequency sweeps measurements of the **G0** to **G4** gels. Top left**.** Log-log frequency sweeps curves at 25 °C. Top right**.** Plot of the storage modulus (G') at 1 Hz *vs.* temperature. Bottom left**.** Plot of G' at 1 Hz *vs.* the **Ox** additives' clogP, at temperatures of 25–80 °C. Dashed lines are guidelines. Bottom right**.** Schematic representation of the possible structural role of oligoesters in the CO-PU three-dimensional network. The scheme is a hypothetical representation based on the experimental data. In the grey ellipsoid is depicted the presence of Ox's entanglements giving physical crosslinking, while the in the orange ellipsoid is depicted the presence of Ox present in the gel main chain/crosslinks. Errors are included in the markers.

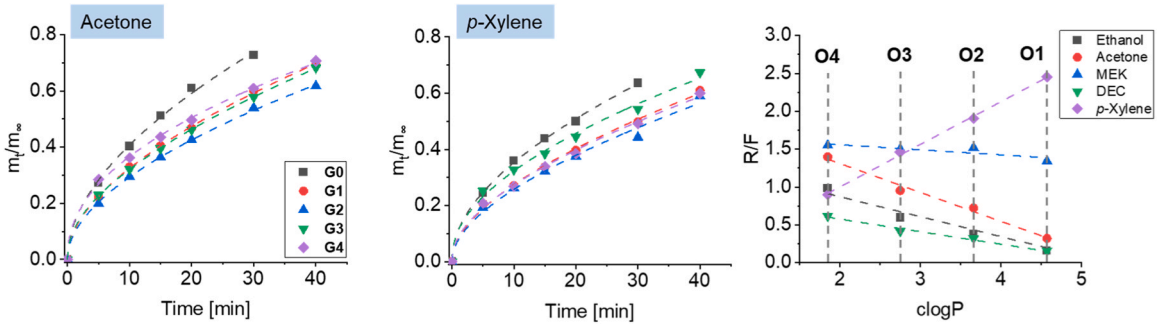


**Fig. 7.** Solvent uptake ($m_t/m_\infty$) *vs.* time for the Co gels **G0** to **G4**, and fitting of the swelling curves to the Peppas-Salhin equation (Eq. 4). Left**.** Swelling in acetone. Centre**.** Swelling in p-xylene. Errors are included in the markers. Right**.** Plots of R/F at swelling equilibrium (180 minutes) *vs.* the clogP of the oligoester additive's **Ox** in the gels. Dashed lines are guidelines. Errors are included in the markers.

tuned to upload a range of different solvents, and to have chain relaxation progressively add to Fickian diffusion during solvent uptake by the gel networks.

Finally, the swollen gels were used to clean a wood panel and glass, removing varnishes and coatings typically found on works of art. These results support a new class of materials with appealing characteristics that advances the state-of-the-art in cleaning tools for Cultural Heritage preservation. Previously reported poly(ethyl) or poly(methyl methacrylate), [51,52] or polyvinyl alcohol-borax gels, had showed good cleaning performances but lack fully sustainable formulation processes and in some case broad solvent compatibility. Recently proposed organogels based on polyhydroxy butyrate and γ-valerolactone, on the other hand, have good "green" profiles but still need optimization of their cleaning efficiency, retentiveness, and mechanical properties [45,92]. While the influence of different isocyanates has been investigated [61], and some components from renewable sources proposed

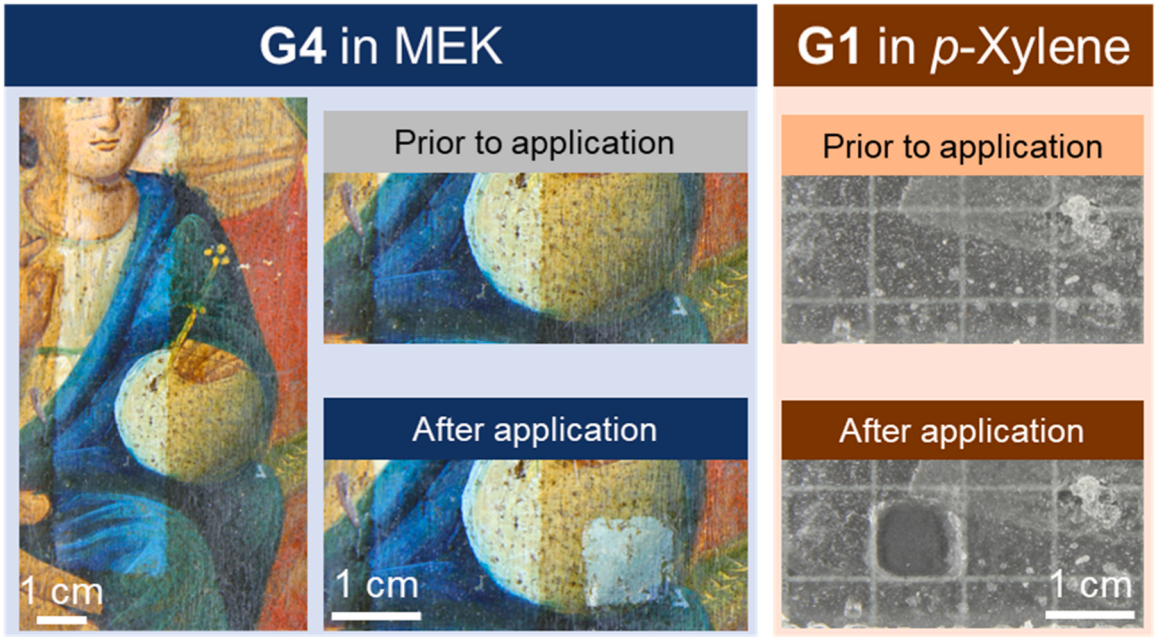


**Fig. 8.** Cleaning tests using the CO-oligoester gels to remove varnish/coating from surfaces. The **G4** gel was swollen in MEK and used to remove a polyhydroxy acid–based varnish from a painted wood panel. The cleaned rectangular stripe aside to the organogel cleaning test, was previously obtained with hydrogels [85] loaded with oil-in-water microemulsions, and kept here as a reference. The **G1** gel was swollen in *p*-xylene and used to remove beeswax from glass. The coated glass is lying on a slab with a grill that serves as spatial reference.

[93,94], we demonstrated here for the first time how bio-derived oligoesters can affect the gelation of CO gels to yield networks with controlled, tunable properties. Polyurethane matrices from castor oil are gaining growing attention to replace petrochemical materials [95], with potential application in fields where sustainable and "green" gel networks are used to confine actives, e.g. food chemistry, cosmetics, biomedicine, agriculture, etc. [96–99], and for engineering foams [100].

## CRediT authorship contribution statement

**D. Bandelli:** Writing – original draft, Methodology, Investigation, Formal analysis, Data curation, Conceptualization. **R. Mastrangelo:** Writing – original draft, Methodology, Investigation, Formal analysis, Data curation. **G. Poggi:** Writing – original draft, Project administration, Methodology, Investigation, Formal analysis, Data curation. **D. Chelazzi:** Writing – review & editing, Writing – original draft, Validation, Supervision, Project administration, Methodology, Formal analysis, Data curation, Conceptualization. **P. Baglioni:** Writing – original draft, Validation, Project administration, Funding acquisition, Formal analysis, Data curation, Conceptualization.

## Declaration of Competing Interest

The authors declare that they have no known competing financial interests or personal relationships that could have appeared to influence the work reported in this paper.

## Data availability

Data will be made available on request.

## Acknowledgements

CSGI and the European Union (GREENART project, Horizon Europe research and innovation program under grant agreement no. 101060941) are gratefully acknowledged for financial support. Views and opinions expressed are however those of the author(s) only and do not necessarily reflect those of the European Union or the European Research Executive Agency (REA). Neither the European Union nor the granting authority can be held responsible for them. DC and DB acknowledge the Project PE 0000020 CHANGES - CUP [SPOKE 7, WP5], NRP Mission 4 Component 2 Investment 1.3, Funded by the European Union – NextGenerationEU for financial support. The publication was made by a researcher (DB) with a research contract funded by the European Union-PNRR NextGenerationEU in accordance with Article 24, paragraph 3a of Law No. 240 of December 30, 2010, as amended and Ministerial Decree No. 1365 of November 8, 2022 and by (RM) with a research contract co-funded by the European Union - PON Research and Innovation 2014–2020 in accordance with Article 24, paragraph 3a of Law No. 240 of December 30, 2010, as amended and Ministerial Decree No. 1062 of August 10, 2021.

## Appendix A. Supporting information

Supplementary data associated with this article can be found in the online version at doi:10.1016/j.colsurfa.2024.134528.

## References

[1] M. Pishvar, R.L. Harne, Foundations for soft, smart matter by active mechanical metamaterials, Adv. Sci. 7 (2020) 2001384.
[2] S. Bahl, H. Nagar, I. Singh, S. Sehgal, Smart materials types, properties and applications: a review, Mater. Today. Proc. 28 (2020) 1302–1306.
[3] Y. Zhang, L. Zhu, J. Tian, L. Zhu, X. Ma, X. He, K. Huang, F. Ren, W. Xu, Smart and functionalized development of nucleic acid-based hydrogels: assembly strategies, Recent Adv. Chall. Adv. Sci. 8 (2021) 2100216.
[4] L. Liu, Y. Zhang, S. Zhang, B. Tang, Advanced phase change materials from natural perspectives: structural design and functional applications, Adv. Sci. 10 (2023) 2207652.
[5] Q. Zhou, Q. Liu, Y. Wang, J. Chen, O. Schmid, M. Rehberg, L. Yang, Bridging Smart Nanosystems with Clinically Relevant Models and Advanced Imaging for Precision Drug Delivery, Advanced Science, n/a 2308659.
[6] X. Wang, M. Shan, S. Zhang, X. Chen, W. Liu, J. Chen, X. Liu, Stimuli-responsive antibacterial materials: molecular structures, Des. Princ. Biomed. Appl. Adv. Sci. 9 (2022) 2104843.
[7] W. Li, E.S. Thian, M. Wang, Z. Wang, L. Ren, Surface design for antibacterial materials: from fundamentals to advanced strategies, Adv. Sci. 8 (2021) 2100368.
[8] H.G. Schild, Poly(N-isopropylacrylamide): experiment, theory and application, Prog. Polym. Sci. 17 (1992) 163–249.

[9] C.-L. Mou, W. Wang, Z.-L. Li, X.-J. Ju, R. Xie, N.-N. Deng, J. Wei, Z. Liu, L.-Y. Chu, Trojan-horse-like stimuli-responsive microcapsules, Adv. Sci. 5 (2018) 1700960.
[10] W. Cai, J. Wang, C. Chu, W. Chen, C. Wu, G. Liu, Metal–organic framework-based stimuli-responsive systems for drug delivery, Adv. Sci. 6 (2019) 1801526.
[11] N. Ono, R. Seishima, K. Okabayashi, H. Imai, S. Fujii, Y. Oaki, Stimuli-responsive sponge for imaging and measuring weak compression stresses, Adv. Sci. 10 (2023) 2206097.
[12] S. Wang, B. Chen, L. Ouyang, D. Wang, J. Tan, Y. Qiao, S. Ge, J. Ruan, A. Zhuang, X. Liu, R. Jia, A novel stimuli-responsive injectable antibacterial hydrogel to achieve synergetic photothermal/gene-targeted therapy towards uveal melanoma, Adv. Sci. 8 (2021) 2004721.
[13] W. Hou, X. Yu, Y. Li, Y. Wei, J. Ren, Ultrafast self-healing, highly stretchable, adhesive, and transparent hydrogel by polymer cluster enhanced double networks for both strain sensors and environmental remediation application, ACS Appl. Mater. Interfaces 14 (2022) 57387–57398.
[14] X. Cao, N. Zhao, R. Li, H. Lv, Z. Zhang, A. Gao, T. Yi, Steric-structure-dependent gel formation, hierarchical structures, rheological behavior, and surface wettability, Chem. Asian J. 11 (2016) 3196–3204.
[15] Z. Yang, L. Chen, D.J. McClements, C. Qiu, C. Li, Z. Zhang, M. Miao, Y. Tian, K. Zhu, Z. Jin, Stimulus-responsive hydrogels in food science: a review, Food Hydrocoll. 124 (2022) 107218.
[16] L. Van Gheluwe, I. Chourpa, C. Gaigne, E. Munnier, Polymer-based smart drug delivery systems for skin application and demonstration of stimuli-responsiveness, Polymers 13 (2021) 1285.
[17] Y. Shymborska, A. Budkowski, J. Raczkowska, V. Donchak, Y. Melnyk, V. Vasiichuk, Y. Stetsyshyn, Switching it Up: the promise of stimuli-responsive polymer systems in biomedical science, Chem. Rec. 24 (2024) e202300217.
[18] L. Zheng, F. Seidi, Y. Liu, W. Wu, H. Xiao, Polymer-based and stimulus-responsive carriers for controlled release of agrochemicals, Eur. Polym. J. 177 (2022) 111432.
[19] S. Amirthalingam, A.K. Rajendran, Y.G. Moon, N.S. Hwang, Stimuli-responsive dynamic hydrogels: design, properties and tissue engineering applications, Mater. Horiz. 10 (2023) 3325–3350.
[20] T. Guaragnone, M. Rossi, D. Chelazzi, R. Mastrangelo, M. Severi, E. Fratini, P. Baglioni, pH-responsive semi-interpenetrated polymer networks of pHEMA/PAA for the capture of copper ions and corrosion removal, ACS Appl. Mater. Interfaces 14 (2022) 7471–7485.
[21] J. Zha, Q. Huang, X. Liu, X. Han, H. Guo, Removal of calcareous concretions from marine archaeological ceramics by means of a stimuli-responsive hydrogel, Polymers 15 (2023) 2929.
[22] G. Cavallaro, S. Milioto, G. Lazzara, Halloysite nanotubes: interfacial properties and applications in cultural heritage, Langmuir 36 (2020) 3677–3689.
[23] R. Castaldo, M.S. de Luna, C. Siviello, G. Gentile, M. Lavorgna, E. Amendola, M. Cocca, On the acid-responsive release of benzotriazole from engineered mesoporous silica nanoparticles for corrosion protection of metal surfaces, J. Cult. Herit. 44 (2020) 317–324.
[24] M.J. Mosquera, R. Zarzuela, M. Luna, Advanced smart materials for preserving concrete heritage buildings, Nat. Rev. Mater. 8 (2023) 74–76.
[25] L. Tortora, G. Di Carlo, M.J. Mosquera, G.M. Ingo, Editorial: Nanoscience and Nanomaterials for the Knowledge and Conservation of Cultural Heritage, in: Frontiers in Materials, 7, 2020.
[26] R. Zarzuela, M. Luna, L.A.M. Carrascosa, M.J. Mosquera, Preserving Cultural Heritage Stone: Innovative Consolidant, Superhydrophobic, Self-Cleaning, and Biocidal Products, in: M. Hosseini, I. Karapanagiotis (Eds.), Advanced Materials for the Conservation of Stone, Springer International Publishing, Cham, 2018, pp. 259–275.
[27] D. Chelazzi, R. Giorgi, P. Baglioni, Microemulsions, Micelles, and functional gels: how colloids and soft matter preserve works of art, Angew. Chem. Int. Ed. 57 (2018) 7296–7303.
[28] D. Chelazzi, P. Baglioni, From nanoparticles to gels: a breakthrough in art conservation science, Langmuir 39 (2023) 10744–10755.
[29] A. Passaretti, L. Cuvillier, G. Sciutto, E. Guilminot, E. Joseph, Biologically derived gels for the cleaning of historical and artistic metal heritage, Appl. Sci. 11 (2021) 3405.
[30] A. Sansonetti, M. Bertasa, C. Canevali, A. Rabbolini, M. Anzani, D. Scalarone, A review in using agar gels for cleaning art surfaces, J. Cult. Herit. 44 (2020) 285–296.
[31] C. Mazzuca, L. Severini, F. Domenici, Y. Toumia, F. Mazzotta, L. Micheli, M. Titubante, B. Di Napoli, G. Paradossi, A. Palleschi, Polyvinyl alcohol based hydrogels as new tunable materials for application in the cultural heritage field, Colloids Surf. B Biointerfaces 188 (2020) 110777.
[32] L. Baij, J. Hermans, B. Ormsby, P. Noble, P. Iedema, K. Keune, A review of solvent action on oil paint, Herit. Sci. 8 (2020) 43.
[33] B. Ormsby, T. Learner, The effects of wet surface cleaning treatments on acrylic emulsion artists' paints – a review of recent scientific research, Stud. Conserv. 54 (2009) 29–41.
[34] B. Ormsby, J. Lee, I. Bonaduce, A. Lluveras-Tenorio, Evaluating Cleaning Systems for Use on Water Sensitive Modern Oil Paints: A Comparative Study, in: K.J. van den Berg, I. Bonaduce, A. Burnstock, B. Ormsby, M. Scharff, L. Carlyle, G. Heydenreich, K. Keune (Eds.), Conservation of Modern Oil Paintings, Springer International Publishing, Cham, 2019, pp. 11–35.
[35] M. Baglioni, R. Mastrangelo, P. Tempesti, T. Ogura, P. Baglioni, Cryogels loaded with nanostructured fluids studied by ultra-small-angle X-ray scattering, Colloids Surf. A Physicochem. Eng. Asp. 660 (2023) 130857.
[36] R. Mastrangelo, C. Resta, E. Carretti, E. Fratini, P. Baglioni, Sponge-like cryogels from liquid–liquid phase separation: structure, porosity, and diffusional gel properties, ACS Appl. Mater. Interfaces 15 (2023) 46428–46439.
[37] R. Mastrangelo, D. Chelazzi, P. Baglioni, New horizons on advanced nanoscale materials for Cultural Heritage conservation, Nanoscale Horiz. (2024).
[38] L. Pensabene Buemi, M.L. Petruzzellis, D. Chelazzi, M. Baglioni, R. Mastrangelo, R. Giorgi, P. Baglioni, Twin-chain polymer networks loaded with nanostructured fluids for the selective removal of a non-original varnish from Picasso's "L'Atelier" at the peggy guggenheim collection, Venice Herit. Sci. 8 (2020) 77.
[39] R. Mastrangelo, D. Chelazzi, G. Poggi, E. Fratini, L. Pensabene Buemi, M. L. Petruzzellis, P. Baglioni, Twin-chain polymer hydrogels based on poly (vinyl alcohol) as new advanced tool for the cleaning of modern and contemporary art, Proc. Natl. Acad. Sci. 117 (2020) 7011–7020.
[40] A. Bartoletti, T. Maor, D. Chelazzi, N. Bonelli, P. Baglioni, L.V. Angelova, B. A. Ormsby, Facilitating the conservation treatment of Eva Hesse's Addendum through practice-based research, including a comparative evaluation of novel cleaning systems, Herit. Sci. 8 (2020) 35.
[41] D. Bandelli, A. Casini, T. Guaragnone, M. Baglioni, R. Mastrangelo, L. Pensabene Buemi, D. Chelazzi, P. Baglioni, Tailoring the properties of poly(vinyl alcohol) "twin-chain" gels via sebacic acid decoration, J. Colloid Interface Sci. 657 (2024) 178–192.
[42] C. Biribicchi, L. Giuliani, A. Macchia, G. Favero, Organogels for low-polar organic solvents: potential applications on cultural heritage materials, Sustainability 15 (2023) 16305.
[43] F. Porpora, L. Dei, T.T. Duncan, F. Olivadese, S. London, B.H. Berrie, R.G. Weiss, E. Carretti, Non-Aqueous poly(dimethylsiloxane) organogel sponges for controlled solvent release: synthesis, characterization, and application in the cleaning of artworks, Gels 9 (2023) 985.
[44] T.T. Duncan, B.H. Berrie, R.G. Weiss, Soft, peelable organogels from partially hydrolyzed poly(vinyl acetate) and benzene-1,4-diboronic acid: applications to clean works of art, ACS Appl. Mater. Interfaces 9 (2017) 28069–28078.
[45] Y. Jia, G. Sciutto, R. Mazzeo, C. Samorì, M.L. Focarete, S. Prati, C. Gualandi, Organogel coupled with microstructured electrospun polymeric nonwovens for the effective cleaning of sensitive surfaces, ACS Appl. Mater. Interfaces 12 (2020) 39620–39629.
[46] A. Casini, D. Chelazzi, P. Baglioni, Advanced methodologies for the cleaning of works of art, Sci. China Technol. Sci. 66 (2023) 2162–2182.
[47] Y. Çakmak, E. Çakmakçi, N.K. Apohan, R. Karadag, Isosorbide, pyrogallol, and limonene-containing thiol-ene photocured bio-based organogels for the cleaning of artworks, J. Cult. Herit. 55 (2022) 391–398.
[48] Y. Jia, G. Sciutto, A. Botteon, C. Conti, M.L. Focarete, C. Gualandi, C. Samorì, S. Prati, R. Mazzeo, Deep eutectic solvent and agar: a new green gel to remove proteinaceous-based varnishes from paintings, J. Cult. Herit. 51 (2021) 138–144.
[49] E. Semenzin, E. Giubilato, E. Badetti, M. Picone, A. Volpi Ghirardini, D. Hristozov, A. Brunelli, A. Marcomini, Guiding the development of sustainable nano-enabled products for the conservation of works of art: proposal for a framework implementing the safe by design concept, Environ. Sci. Pollut. Res. 26 (2019) 26146–26158.
[50] A. Elnaggar, Nine principles of green heritage science: life cycle assessment as a tool enabling green transformation, Herit. Sci. 12 (2024) 7.
[51] M.D. Pianorsi, M. Raudino, N. Bonelli, D. Chelazzi, R. Giorgi, E. Fratini, P. Baglioni, Organogels for the cleaning of artifacts, Pure Appl. Chem. 89 (2017) 3–17.
[52] P. Ferrari, D. Chelazzi, N. Bonelli, A. Mirabile, R. Giorgi, P. Baglioni, Alkyl carbonate solvents confined in poly (ethyl methacrylate) organogels for the removal of pressure sensitive tapes (PSTs) from contemporary drawings, J. Cult. Herit. 34 (2018) 227–236.
[53] P. Baglioni, N. Bonelli, D. Chelazzi, A. Chevalier, L. Dei, J. Domingues, E. Fratini, R. Giorgi, M. Martin, Organogel formulations for the cleaning of easel paintings, Appl. Phys. A 121 (2015) 857–868.
[54] I. Chakraborty, K. Chatterjee, Polymers and composites derived from castor oil as sustainable materials and degradable biomaterials: current status and emerging trends, Biomacromolecules 21 (2020) 4639–4662.
[55] M.A.R. Meier, J.O. Metzger, U.S. Schubert, Plant oil renewable resources as green alternatives in polymer science, Chem. Soc. Rev. 36 (2007) 1788–1802.
[56] L. Pari, E. Alexopoulou, W. Stefanoni, F. Latterini, C. Cavalaris, N. Palmieri, The eco-efficiency of castor supply chain: a greek case study, Agriculture 12 (2022) 206.
[57] B.D. Neimark, T.M. Healy, Small-scale commodity frontiers: the bioeconomy value chain of castor oil in Madagascar, J. Agrar. Change 18 (2018) 632–657.
[58] L. Carrino, D. Visconti, N. Fiorentino, M. Fagnano, Biofuel production with castor bean: a win–win strategy for marginal land, Agronomy 10 (2020) 1690.
[59] P. Berman, S. Nizri, Z. Wiesman, Castor oil biodiesel and its blends as alternative fuel, Biomass-.-. Bioenergy 35 (2011) 2861–2866.
[60] Z.S. Petrović, D. Fajnik, Preparation and properties of castor oil-based polyurethanes, J. Appl. Polym. Sci. 29 (1984) 1031–1040.
[61] E. Hablot, D. Zheng, M. Bouquey, L. Avérous, Polyurethanes based on castor oil: kinetics, chemical, mechanical and thermal properties, Macromol. Mater. Eng. 293 (2008) 922–929.
[62] N. Karak, S. Rana, J.W. Cho, Synthesis and characterization of castor-oil-modified hyperbranched polyurethanes, J. Appl. Polym. Sci. 112 (2009) 736–743.
[63] G. Poggi, H.D. Santan, J. Smets, D. Chelazzi, D. Noferini, M.L. Petruzzellis, L. Pensabene Buemi, E. Fratini, P. Baglioni, Nanostructured bio-based castor oil organogels for the cleaning of artworks, J. Colloid Interface Sci. 638 (2023) 363–374.

[64] A. Zuliani, D. Bandelli, D. Chelazzi, R. Giorgi, P. Baglioni, Environmentally friendly ZnO/Castor oil polyurethane composites for the gas-phase adsorption of acetic acid, J. Colloid Interface Sci. 614 (2022) 451–459.
[65] A. Zuliani, M. Rapisarda, D. Chelazzi, P. Baglioni, P. Rizzarelli, Synthesis, characterization, and soil burial degradation of biobased polyurethanes, Polymers 14 (2022) 4948.
[66] D. Bandelli, R. Mastrangelo, G. Poggi, D. Chelazzi, P. Baglioni, New sustainable polymers and oligomers for cultural heritage conservation, Chem. Sci. 15 (2024) 2443–2455.
[67] T. Sander, J. Freyss, M. von Korff, C. Rufener, DataWarrior: an open-source program for chemistry aware data visualization and analysis, J. Chem. Inf. Model. 55 (2015) 460–473.
[68] L. Sangroniz, M. Safari, A. Martínez de Ilarduya, H. Sardon, D. Cavallo, A. J. Müller, Disappearance of melt memory effect with comonomer incorporation in isodimorphic random copolyesters, Macromolecules 56 (2023) 7879–7888.
[69] D. Bandelli, I. Muljajew, K. Scheuer, J.B. Max, C. Weber, F.H. Schacher, K. D. Jandt, U.S. Schubert, Copolymerization of caprolactone isomers to obtain nanoparticles with constant hydrophobicity and tunable crystallinity, Macromolecules 53 (2020) 5208–5217.
[70] D. Bandelli, J. Alex, C. Helbing, N. Ueberschaar, H. Görls, P. Bellstedt, C. Weber, K.D. Jandt, U.S. Schubert, Poly(3-ethylglycolide): a well-defined polyester matching the hydrophilic hydrophobic balance of PLA, Polym. Chem. 10 (2019) 5440–5451.
[71] K. Scheuer, D. Bandelli, C. Helbing, C. Weber, J. Alex, J.B. Max, A. Hocken, O. Stranik, L. Seiler, F. Gladigau, U. Neugebauer, F.H. Schacher, U.S. Schubert, K. D. Jandt, Self-assembly of copolyesters into stereocomplex crystallites tunes the properties of polyester nanoparticles, Macromolecules 53 (2020) 8340–8351.
[72] M. Shibayama, T. Tanaka, C.C. Han, Small angle neutron scattering study on poly (N-isopropyl acrylamide) gels near their volume-phase transition temperature, J. Chem. Phys. 97 (1992) 6829–6841.
[73] C.M. Roland, Viscoelastic Behavior of Rubbery Materials, OUP Oxford, 2011.
[74] I.M. Ward, J. Sweeney, Mechanical Properties of Solid Polymers, John Wiley & Sons, 2012.
[75] A.M. Fenton, R. Xie, M.P. Aplan, Y. Lee, M.G. Gill, R. Fair, F. Kempe, M. Sommer, C.R. Snyder, E.D. Gomez, R.H. Colby, Predicting the plateau modulus from molecular parameters of conjugated polymers, ACS Cent. Sci. 8 (2022) 268–274.
[76] C.A. García-Franco, B.A. Harrington, D.J. Lohse, On the rheology of ethylene-octene copolymers, Rheol. Acta 44 (2005) 591–599.
[77] A.V. Kaliyathan, A.V. Rane, S. Jackson, S. Thomas, Analysis of diffusion characteristics for aromatic solvents through carbon black filled natural rubber/butadiene rubber blends, Polym. Compos. 42 (2021) 375–396.
[78] P.M. Visakh, S. Thomas, K. Oksman, A.P. Mathew, Cellulose nanofibres and cellulose nanowhiskers based natural rubber composites: diffusion, sorption, and permeation of aromatic organic solvents, J. Appl. Polym. Sci. 124 (2012) 1614–1623.
[79] P.P. Vijayan, M.G. Harikrishnan, D. Puglia, P.P. Vijayan, J.M. Kenny, S. Thomas, Solvent uptake of liquid rubber toughened epoxy/clay nanocomposites, Adv. Polym. Technol. 35 (2016).
[80] N.A. Peppas, J.J. Sahlin, A simple equation for the description of solute release. III. Coupling of diffusion and relaxation, Int. J. Pharm. 57 (1989) 169–172.
[81] A. Aluigi, M. Ballestri, A. Guerrini, G. Sotgiu, C. Ferroni, F. Corticelli, M. B. Gariboldi, E. Monti, G. Varchi, Organic solvent-free preparation of keratin nanoparticles as doxorubicin carriers for antitumour activity, Mater. Sci. Eng. C 90 (2018) 476–484.
[82] G. Maurizii, S. Moroni, J.V. Jimènez Núnez, G. Curzi, M. Tiboni, A. Aluigi, L. Casettari, Non-invasive peptides delivery using chitosan nanoparticles assembled via scalable microfluidic technology, Carbohydr. Polym. Technol. Appl. 7 (2024) 100424.
[83] J.-P. Simonin, On the comparison of pseudo-first order and pseudo-second order rate laws in the modeling of adsorption kinetics, Chem. Eng. J. 300 (2016) 254–263.
[84] Y.S. Ho, G. McKay, Pseudo-second order model for sorption processes, Process Biochem. 34 (1999) 451–465.
[85] M. Baglioni, J.A.L. Domingues, E. Carretti, E. Fratini, D. Chelazzi, R. Giorgi, P. Baglioni, Complex fluids confined into semi-interpenetrated chemical hydrogels for the cleaning of classic art: a rheological and SAXS study, ACS Appl. Mater. Interfaces 10 (2018) 19162–19172.
[86] T. Poli, A. Piccirillo, M. Nervo, O. Chiantore, Interactions of natural resins and pigments in works of art, J. Colloid Interface Sci. 503 (2017) 1–9.
[87] P. Vandenabeele, B. Wehling, L. Moens, H. Edwards, M. De Reu, G. Van Hooydonk, Analysis with micro-Raman spectroscopy of natural organic binding media and varnishes used in art, Anal. Chim. Acta 407 (2000) 261–274.
[88] M. Durbán García, T. Espejo Arias, A.M. López Montes, Md.R. Blanc García, The behavior of different varnishes applied to graphic artworks: comparison using a methodological protocol, Stud. Conserv. 67 (2022) 603–611.
[89] S. Cather, H. Howard, The use of wax and wax-resin preservatives on English mediaeval wall paintings: rationale and consequences, Stud. Conserv. 31 (1986) 48–53.
[90] D. Pinna, S. Bracci, D. Magrini, B. Salvadori, A. Andreotti, M.P. Colombini, Deterioration and discoloration of historical protective treatments on marble, Environ. Sci. Pollut. Res. 29 (2022) 20694–20710.
[91] A. Pan, S. Chiussi, P. González, J. Serra, B. León, Comparative evaluation of UV–vis–IR Nd:YAG laser cleaning of beeswax layers on granite substrates, Appl. Surf. Sci. 257 (2011) 5484–5490.
[92] C. Samorì, P. Galletti, L. Giorgini, R. Mazzeo, L. Mazzocchetti, S. Prati, G. Sciutto, F. Volpi, E. Tagliavini, The green attitude in art conservation: polyhydroxybutyrate–based gels for the cleaning of oil paintings, ChemistrySelect 1 (2016) 4502–4508.
[93] M.A. Corcuera, L. Rueda, B. Fernandez d'Arlas, A. Arbelaiz, C. Marieta, I. Mondragon, A. Eceiza, Microstructure and properties of polyurethanes derived from castor oil, Polym. Degrad. Stab. 95 (2010) 2175–2184.
[94] H. Yeganeh, P. Hojati-Talemi, Preparation and properties of novel biodegradable polyurethane networks based on castor oil and poly(ethylene glycol), Polym. Degrad. Stab. 92 (2007) 480–489.
[95] S.S. Panda, B.P. Panda, S.K. Nayak, S. Mohanty, A review on waterborne thermosetting polyurethane coatings based on castor oil: synthesis, characterization, and application, Polym. Plast. Technol. Eng. 57 (2018) 500–522.
[96] J.E. Norton, Y. Gonzalez Espinosa, R.L. Watson, F. Spyropoulos, I.T. Norton, Functional food microstructures for macronutrient release and delivery, Food Funct. 6 (2015) 663–678.
[97] R. Macoon, T. Guerriero, A. Chauhan, Extended release of dexamethasone from oleogel based rods, J. Colloid Interface Sci. 555 (2019) 331–341.
[98] J. Zhang, Y. Wang, Q. Wei, M. Li, X. Chen, 3D printable, stretchable, anti-freezing and rapid self-healing organogel-based sensors for human motion detection, J. Colloid Interface Sci. 653 (2024) 1514–1525.
[99] G.L. Zabot, F. Schaefer Rodrigues, L. Polano Ody, M. Vinícius Tres, E. Herrera, H. Palacin, J.S. Córdova-Ramos, I. Best, L. Olivera-Montenegro, Encapsulation of bioactive compounds for food and agricultural applications, Polymers 14 (2022) 4194.
[100] J. Lavazza, Q. Zhang, C. de Kergariou, G. Comandini, W.H. Briscoe, J. L. Rowlandson, T.H. Panzera, F. Scarpa, Rigid polyurethane foams from commercial castor oil resins, Polym. Test. 135 (2024) 108457.